AD-A079 325 OHIO STATE UNIV COLUMBUS ELECTROSCIENCE LAB F/G 20/14
RESEARCH ON NEAR FIELD PATTERN EFFECTS.(U)
NOV 79 N WANG, W D BURNSIDE N00019-78-C-0524
UNCLASSIFIED ESL-711305-4 NL

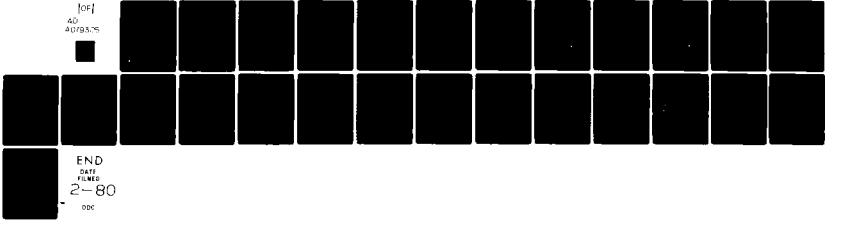

END
DATE FILMED
2-80
DDC

OSU

The Ohio State University

# RESEARCH ON NEAR FIELD PATTERN EFFECTS

N. Wang and W. D. Burnside

LEVEL II

APPROVED FOR PUBLIC RELEASE;
DISTRIBUTION UNLIMITED



The Ohio State University

**ElectroScience Laboratory**

Department of Electrical Engineering
Columbus, Ohio 43212

FINAL REPORT 711305-4

November 1979

Contract N00019-78-C-0524



Department of the Navy
Naval Air Systems Command
Washington, D.C. 20361

## NOTICES

When Government drawings, specifications, or other data are used for any purpose other than in connection with a definitely related Government procurement operation, the United States Government thereby incurs no responsibility nor any obligation whatsoever, and the fact that the Government may have formulated, furnished, or in any way supplied the said drawings, specifications, or other data, is not to be regarded by implication or otherwise as in any manner licensing the holder or any other person or corporation, or conveying any rights or permission to manufacture, use, or sell any patented invention that may in any way be related thereto.

UNCLASSIFIED

SECURITY CLASSIFICATION OF THIS PAGE *(When Data Entered)*

| REPORT DOCUMENTATION PAGE | | READ INSTRUCTIONS BEFORE COMPLETING FORM |
|---|---|---|
| 1. REPORT NUMBER | 2. GOVT ACCESSION NO. | 3. RECIPIENT'S CATALOG NUMBER |
| 4. TITLE *(and Subtitle)* (6) RESEARCH ON NEAR FIELD PATTERN EFFECTS. | | 5. TYPE OF REPORT & PERIOD COVERED (7) Final Report. |
| | | 6. PERFORMING ORG. REPORT NUMBER (14) ESL-711305-4 |
| 7. AUTHOR(s) (10) N. Wang and W. D. Burnside | | 8. CONTRACT OR GRANT NUMBER(s) (15) Contract N00019-78-C-0524 |
| 9. PERFORMING ORGANIZATION NAME AND ADDRESS The Ohio State University ElectroScience Laboratory, Department of Electrical Engineering Columbus, Ohio, 43212 | | 10. PROGRAM ELEMENT, PROJECT, TASK AREA & WORK UNIT NUMBERS 12971 |
| 11. CONTROLLING OFFICE NAME AND ADDRESS Department of the Navy Naval Air Systems Command Washington, D.C. 20361 | | (11) 12. REPORT DATE November 1979 |
| | | 13. NUMBER OF PAGES 24 |
| 14. MONITORING AGENCY NAME & ADDRESS *(if different from Controlling Office)* | | 15. SECURITY CLASS. *(of this report)* Unclassified |
| | | 15a. DECLASSIFICATION/DOWNGRADING SCHEDULE |

16. DISTRIBUTION STATEMENT *(of this Report)*

**APPROVED FOR PUBLIC RELEASE;**
**DISTRIBUTION UNLIMITED**

17. DISTRIBUTION STATEMENT *(of the abstract entered in Block 20, if different from Report)*

18. SUPPLEMENTARY NOTES

19. KEY WORDS *(Continue on reverse side if necessary and identify by block number)*

Near fields
Electromagnetic radiation
High frequency solutions
Airborne antennas
Geodesic
Prolate spheroid
Aircraft model
Multiple plate simulation

20. ABSTRACT *(Continue on reverse side if necessary and identify by block number)*

Under the present contract, a simple and efficient multiple-plate model has been developed for the aircraft substructures. Using this model, the tail, wings, stabilizer and engine housings can be easily simulated. A three dimensional model (i.e., prolate spheroid) is employed for investigating the radiation from an aircraft fuselage. In addition, high frequency solutions for the electric field due to antennas radiating from a perfectly conducting convex body are developed. The expressions are given in terms of a fixed ray coordinate system which follows the

DD FORM 1 JAN 73 1473 EDITION OF 1 NOV 65 IS OBSOLETE

412 251

UNCLASSIFIED

SECURITY CLASSIFICATION OF THIS PAGE *(When Data Entered)*

JCP

A

20.

geodesic path on the conducting surface. These expressions are simple, compact, and are given in terms of some well known and tabulated Fock integrals. Furthermore, these expressions reduce to the geometrical optics solution in the "deep" lit region and recover the Keller's surface ray representation in the deep shadow region. The continuity of the fields across the shadow boundary is also established. A major task of applying the high frequency solution to solve practical problems, (namely, determining the unique geodesic path on the conducting surface), is also accomplished in the case of a prolate spheroid. Numerical results obtained by employing the newly developed solution are in good agreement with eigenfunction solutions and measured results.

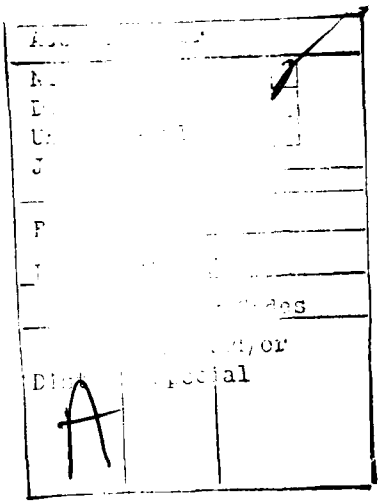

# I. SUMMARY OF RESEARCH

Under a previous contract (N00019-77-C-0299) an aircraft simulation model was developed for the analysis of near field pattern effects due to an airborne antenna. The solution was based on the geometrical theory of diffraction (GTD). That model treated the fuselage as a composite elliptic cylinder and the wings and stabilizers as finite flat plates. The near field formulation developed has been used to calculate the radiation patterns in and close to the roll and elevation planes of the aircraft. The numerical results obtained were in excellent agreement with the measured patterns[1].

However as the previous solution was used to analyze various private, commercial and military aircraft, it became apparent that our simple aircraft model was unable to simulate the arbitrary sub-structures of the aircraft, such as T-tails, jet engine-housing, and numerous structures being attached to the basic fuselage and wings. For these reasons, the previous solution was extended under the present contract (N00019-78-C-0524) in terms of a multiple plate model[2] for the aircraft substructures. This multiple plate approach allows one to model the various substructures by boxing-out the structure using a set of finite flat plates. The finite flat plates are chosen to be the basic building blocks to simulate these substructures in that they are easy to input in the computer code and are efficient to analyze. The basic concept of the multiple plate model is described here and one specific example is used to demonstrate its validity. More numerical results with accompanying measurements can be found in the first quarterly report[2].

Consider a bent plate attached to a circular cylinder as shown in Figure 1. The source, a monopole antenna, is located at Q'. The various rays contributing to the radiation pattern are illustrated

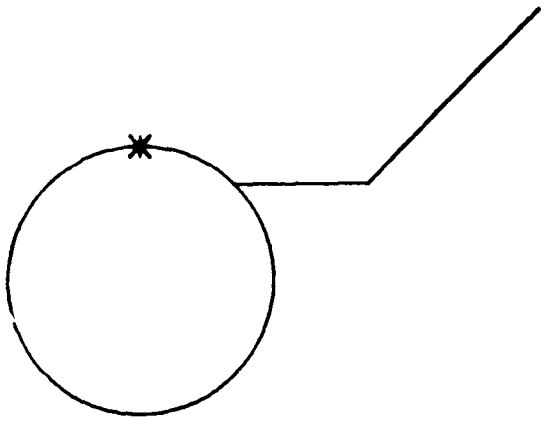

Figure 1. A bent plate attached to a circular cylinder.

in Figure 2. Note that in the present solution higher-order terms are included in the analysis. The source, reflected, and diffracted terms used in our previous solution[1] are shown in Figure 3. The superimposed pattern using these three GTD terms is illustrated in Figure 3d. One should note the disconinuities in this pattern at $\underset{\sim}{\sim} 14^{o}$ and $45^{o}$. These discontinuities are compensated for by the higher-order GTD interaction terms illustrated in Figure 4. As before, these terms are plotted relative to the same signal level such that one can observe their relative significance. It is clear that these higher-order terms can be significant in certain sectors of the pattern. In order to demonstrate how the complete GTD solution creates the desired total pattern, various combinations of terms are illustrted in Figure 5. The geometrical optics solution is shown in Figure 5b and, as before, several discontinuities exist in this pattern. The total superposition of the recently introduced higher-order terms is shown in Figure 5c. It is very interesting that the patterns illustrated in Figure 3d and 5c superimpose to give the smooth total pattern shown in Figure 5d. As with any GTD solution for a complex structure, one can compute even higher order terms. However, there are two major problems with adding such terms beyond those included here: 1) the accuracy of the GTD diffraction solutions become questionable, 2) the numerical solution

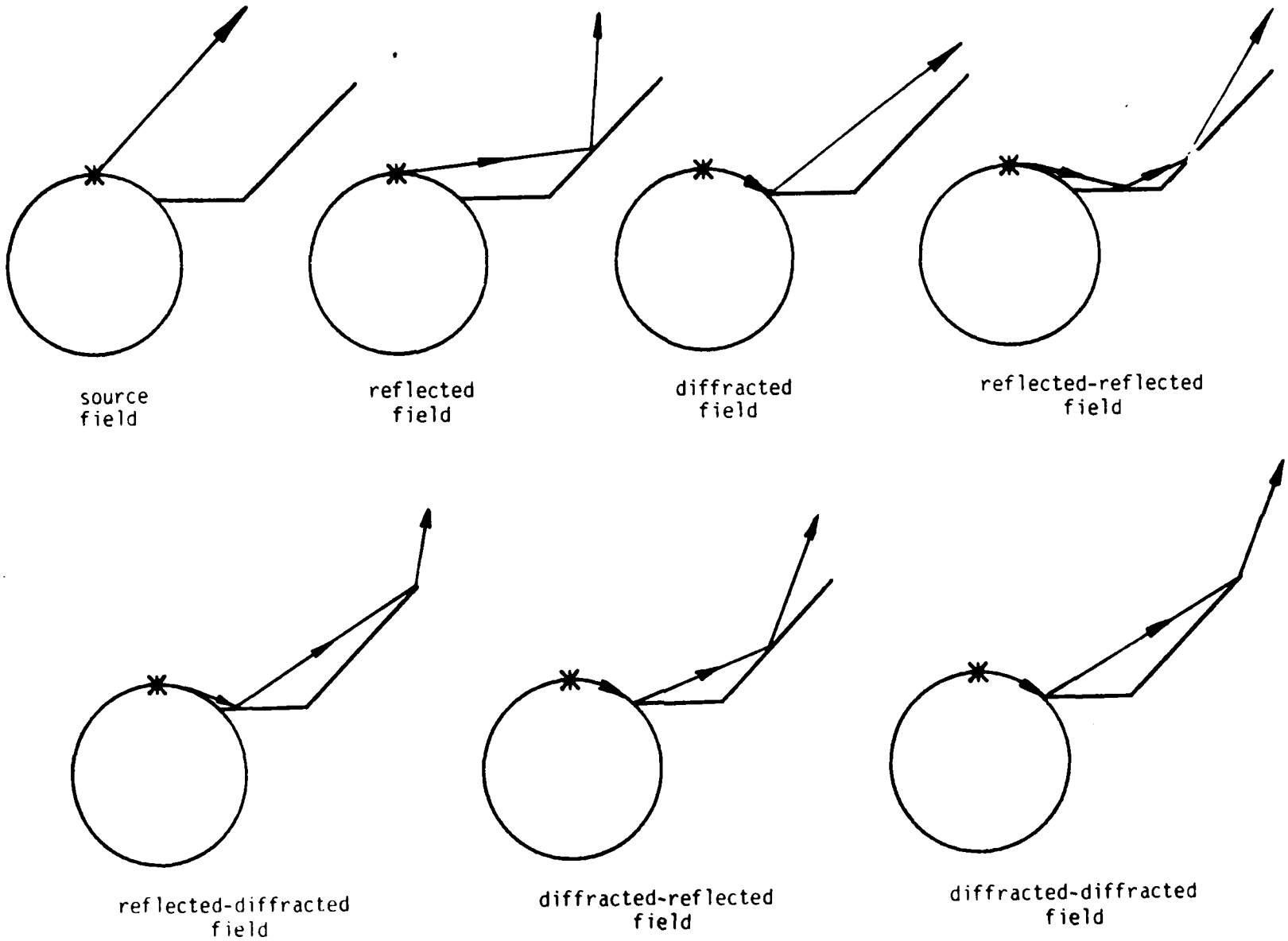


Figure 2. Various GTD terms.

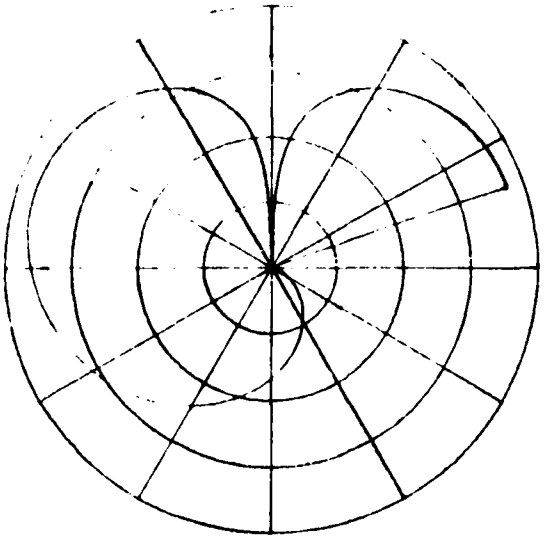

(a) source field (S)

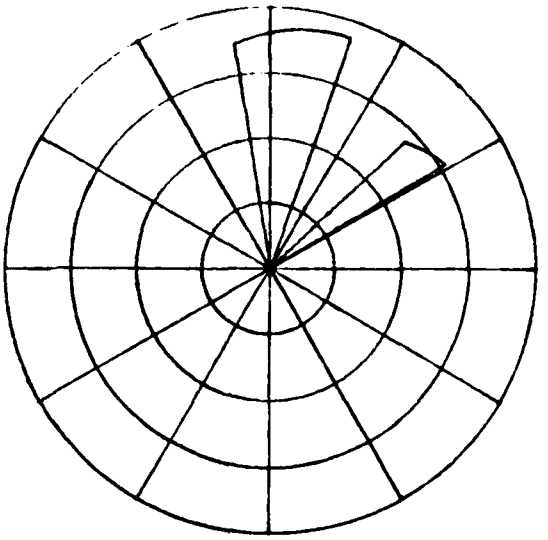

(b) reflected field (R)

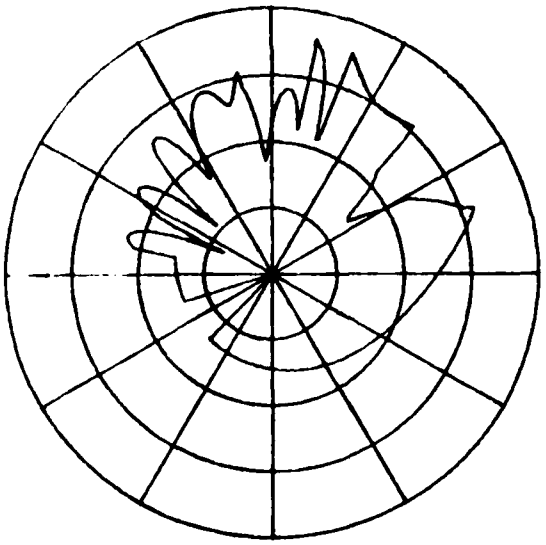

(c) diffracted field (D)

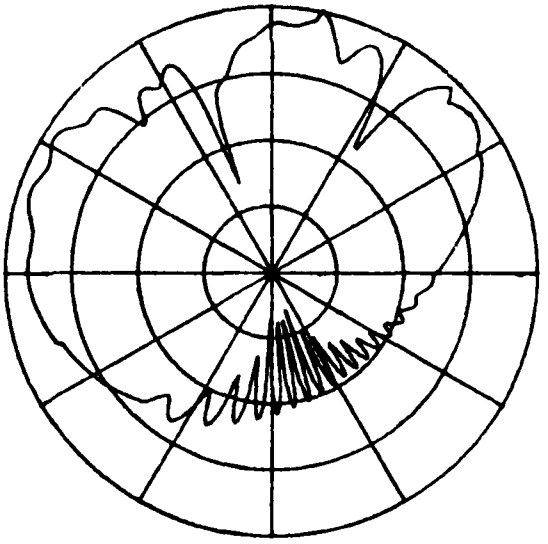

(d) S + R + D

Figure 3. Radiation patterns due to various GTD terms.

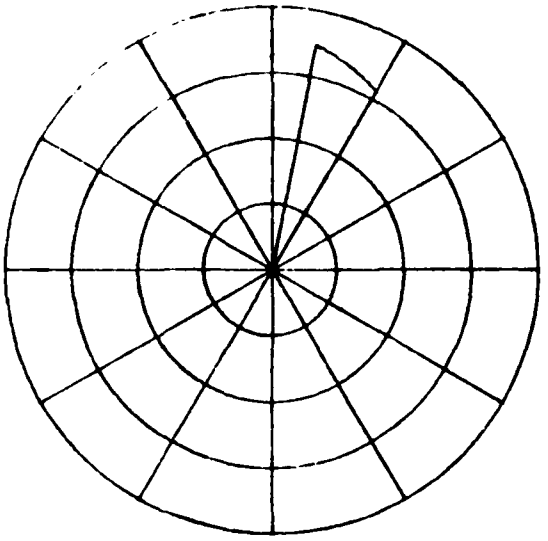

(a) reflected/reflected fields (R/R)

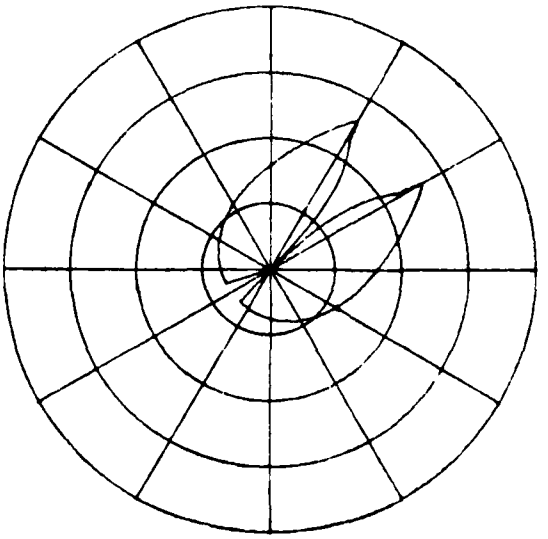

(b) reflected/diffracted field (R/D)

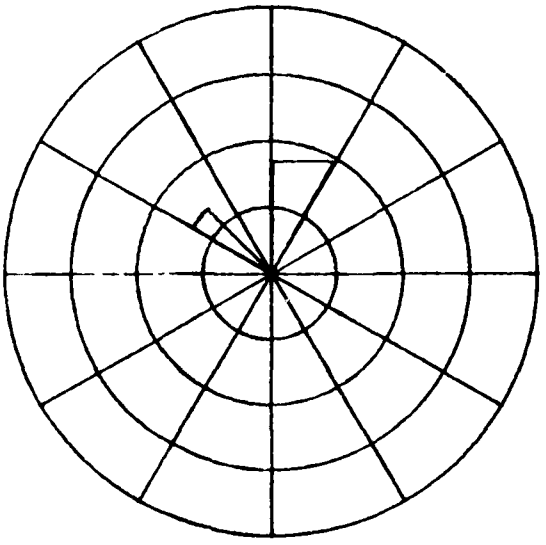

(c) diffracted/reflected field (D/R)

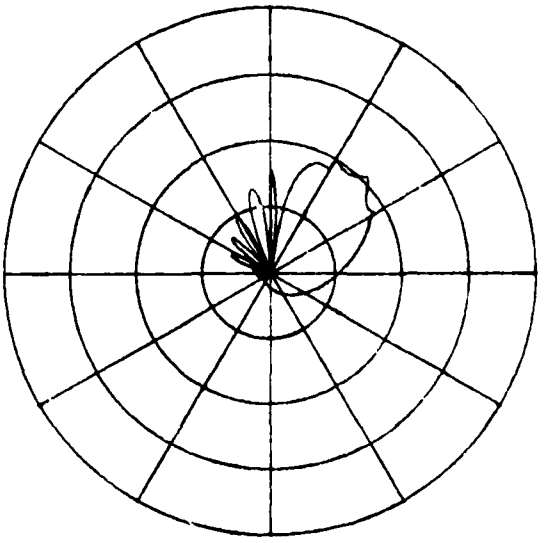

(d) diffracted/diffracted field (D/D)

Figure 4. Radiation patterns due to the second order interaction GTD terms.

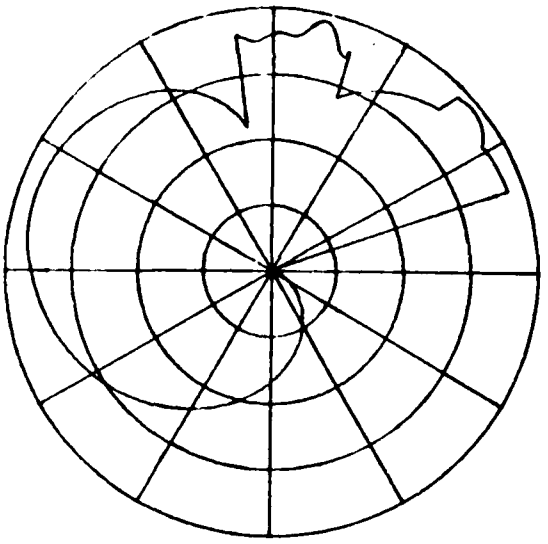

(a) S + R

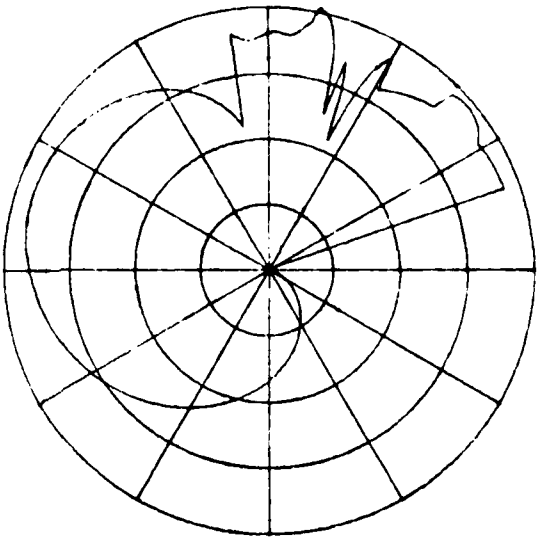

(b) geometric optics solution. (S + R + RR)

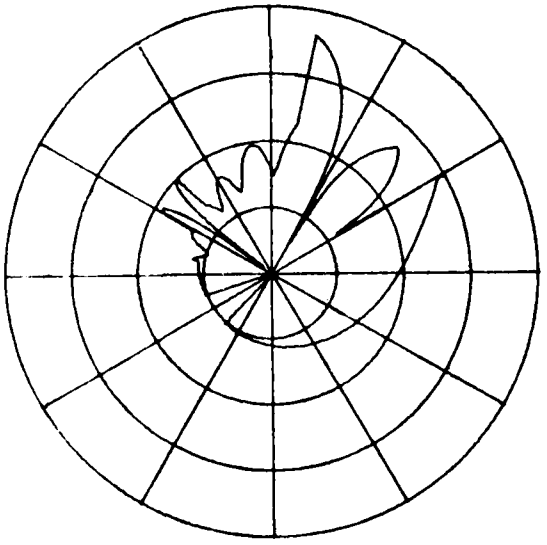

(c) second order interaction GTD terms. (R/R + R/D + D/R + D/D)

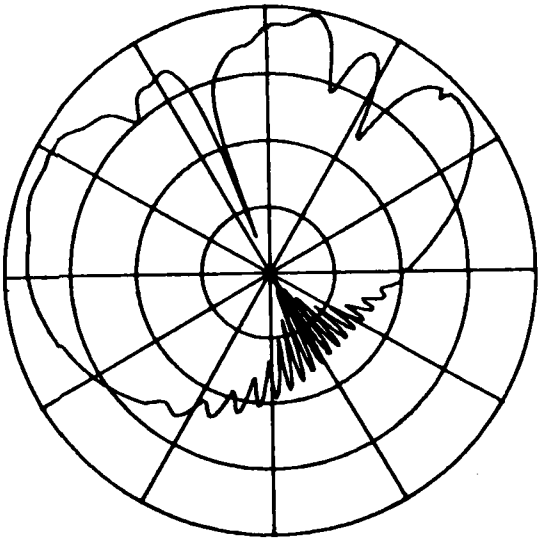

(d) total solution.

Figure 5. Radiation patterns due to various combinations of the GTD terms.

becomes very inefficient. Furthermore based on cases examined to date, it appears that the major structures found on aircraft can be adequately solved using the interaction terms considered here. In order to illustrate the various GTD mechanisms they are all shown in Figure 2 in terms of ray paths. The previous example was used to illustrate the various GTD terms included in the present analysis. The next example is used to demonstrate the validity of the present solution.

The geometry illustrated in Figure 6 is included in that it tends to resemble a more realistic aircraft configuration. The roll plane measured and calculated patterns are shown in Figure 7. Two sets of measured and calculated patterns are illustrated in Figures 8 and 9 for $68^{o}$ and $112^{o}$ conical pattern cuts. In each case both the $E_{\theta}$ and $E_{\phi}$ components of the near zone field are plotted relative to the same radiation level. In addition there is very good agreement between calculated and measured patterns. The above patterns are presented to illustrate the fact that our numerical solutions can solve the proposed type of airborne antenna problem.

A second aspect of our analysis of airborne antenna patterns under the present contract is to investigate ways to analyze the complete near field volumetric pattern. In order to accomplish this goal, the first step is to adopt a three dimensional model for the aircraft fuselage. The model must provide a good approximate shape for the fuselage in the antenna studies not only in the neighborhood of the roll and elevation planes but also in the regions close to the nose and tail of the aircraft. Furthermore, the model must be efficient and of a form that it can be adopted for the fuselage-wing analysis, i.e., finite flat plates can be easily attached to allow the studies of fuselage-wing interaction. In this report, a surface of revolution model (namely, a prolate spheroid) is chosen to simulate the aircraft fuselage. Unlike the previous composite cylinder model, the prolate spheroid is a doubly-curved surface with finite principal radii of curvature and is apparently a better approximation for the fuselage.

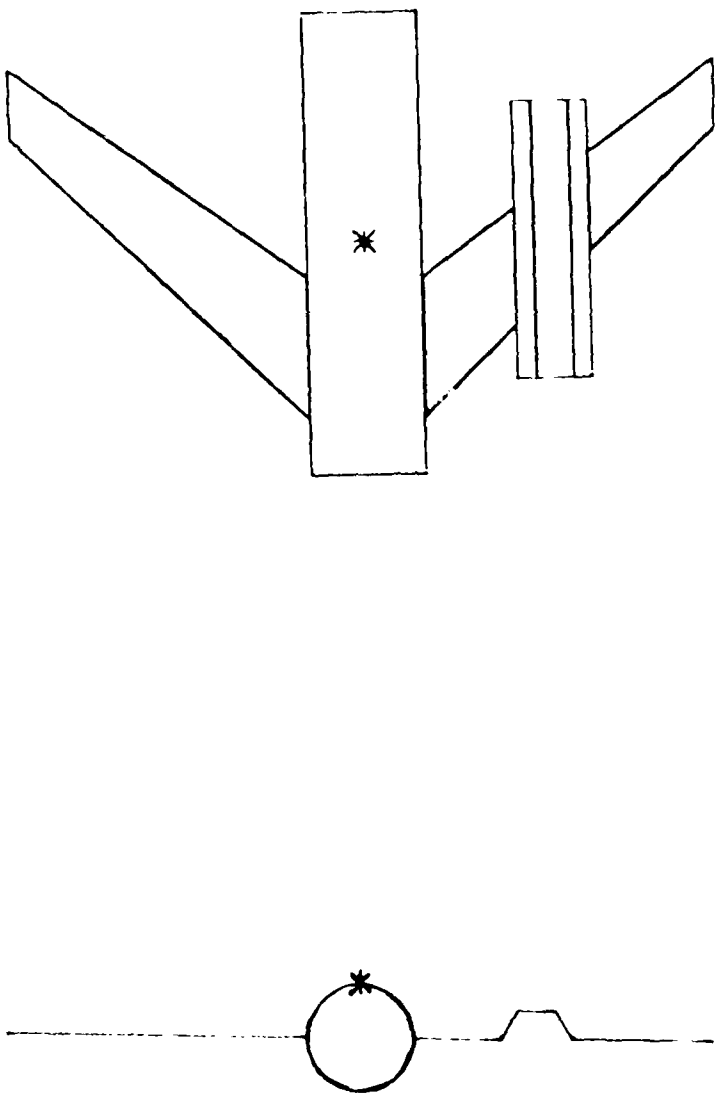

Figure 6. Test geometry with flat-plate engine model.

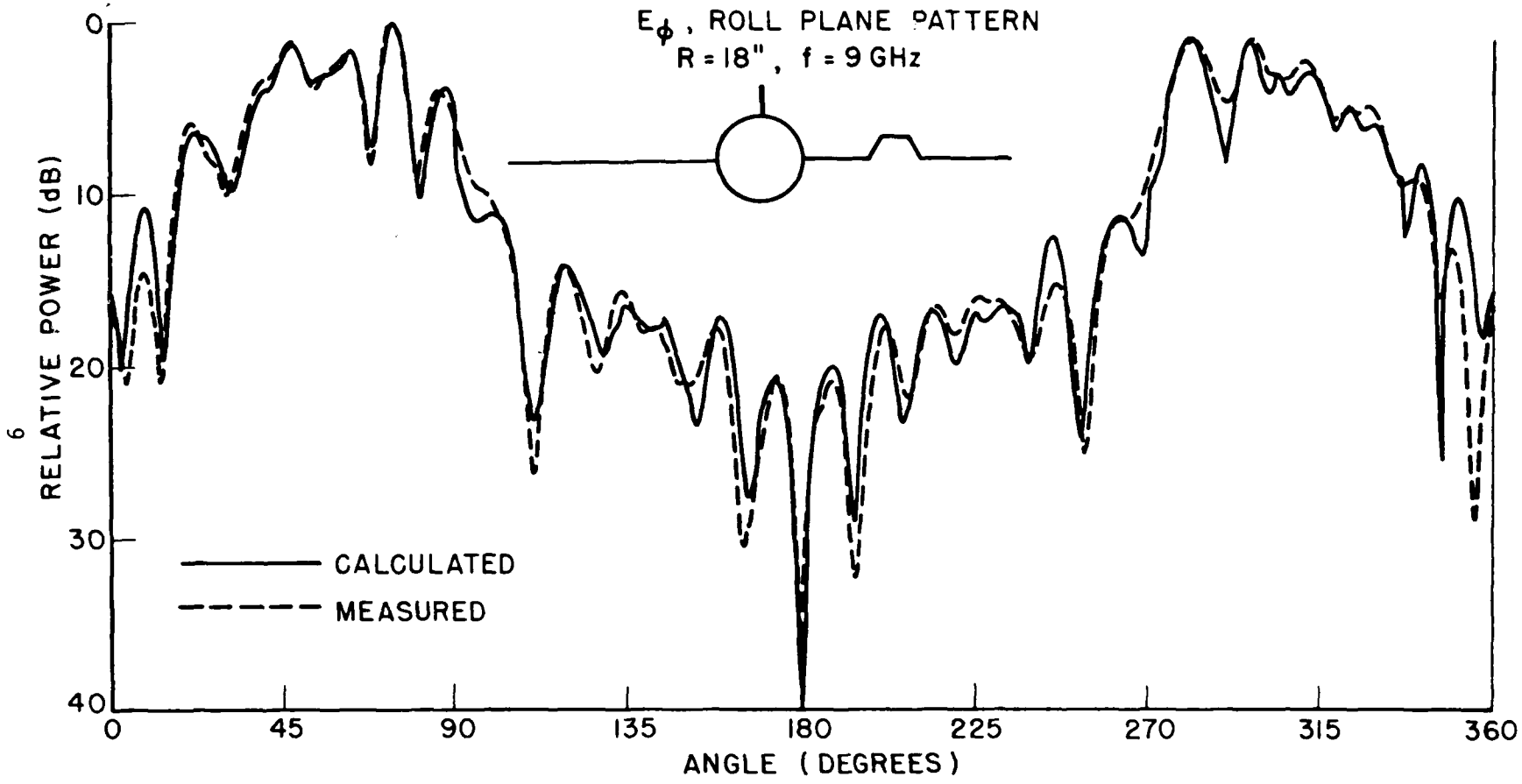


Figure 7. Comparison of measured and calculated near-field pattern for the test geometry shown.

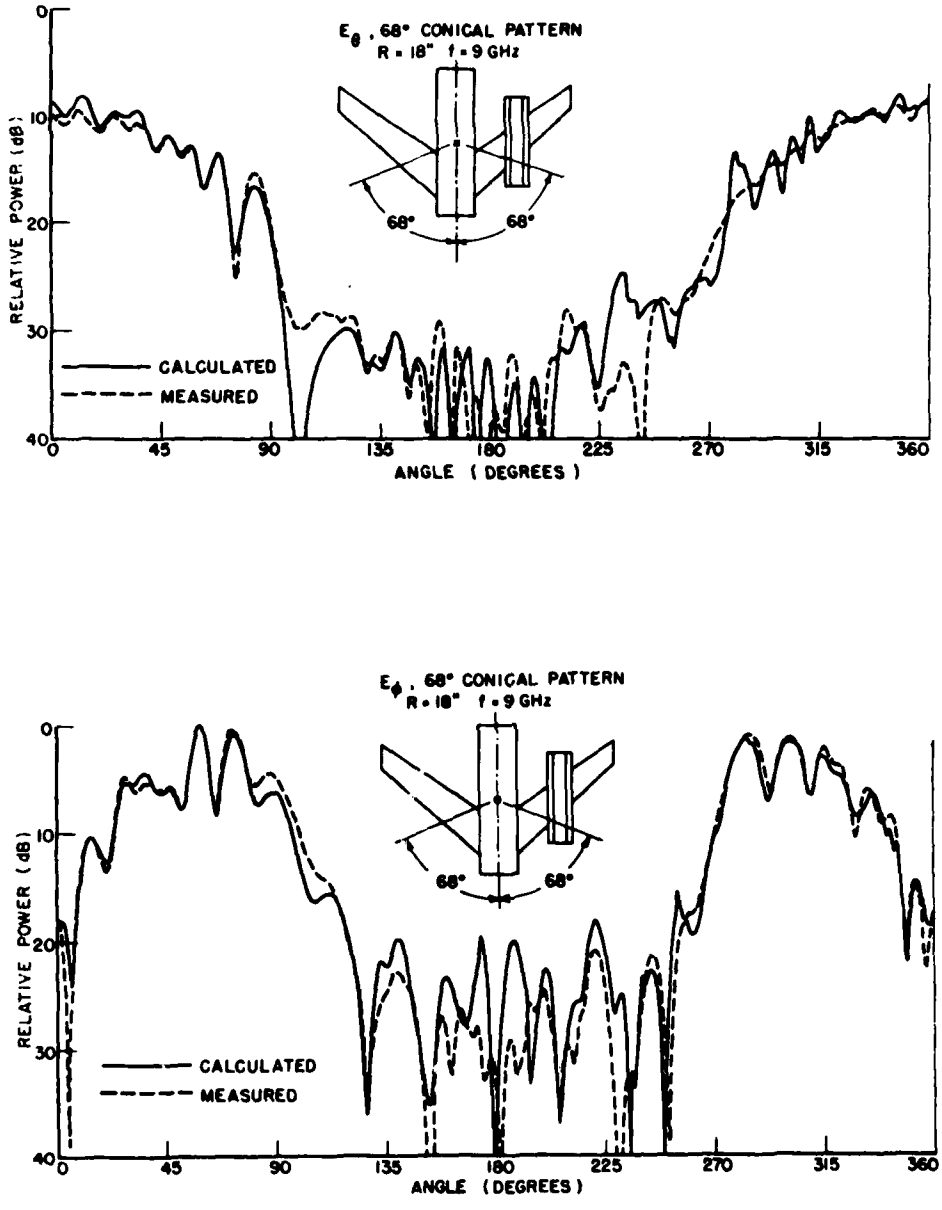


Figure 8. Comparison of measured and calculated near-field patterns for the test geometry. Note that the engine is simulated by flat plates.

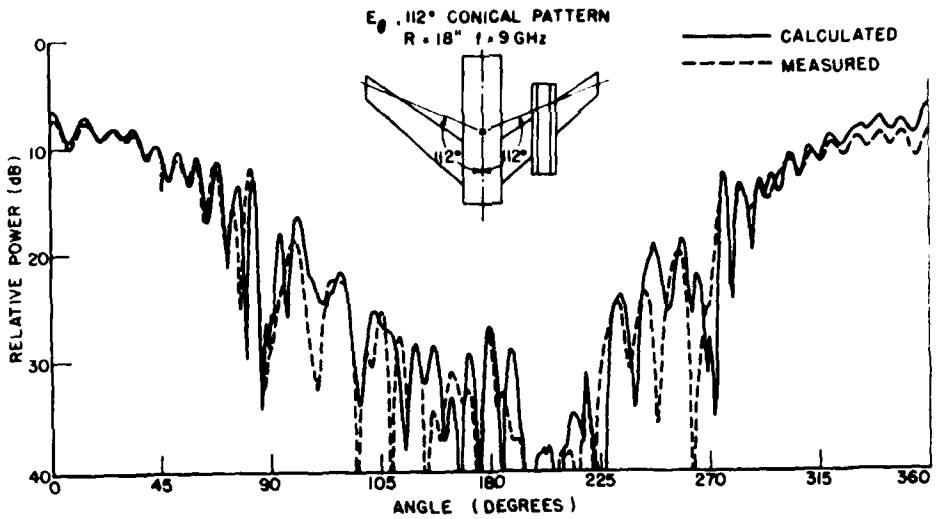


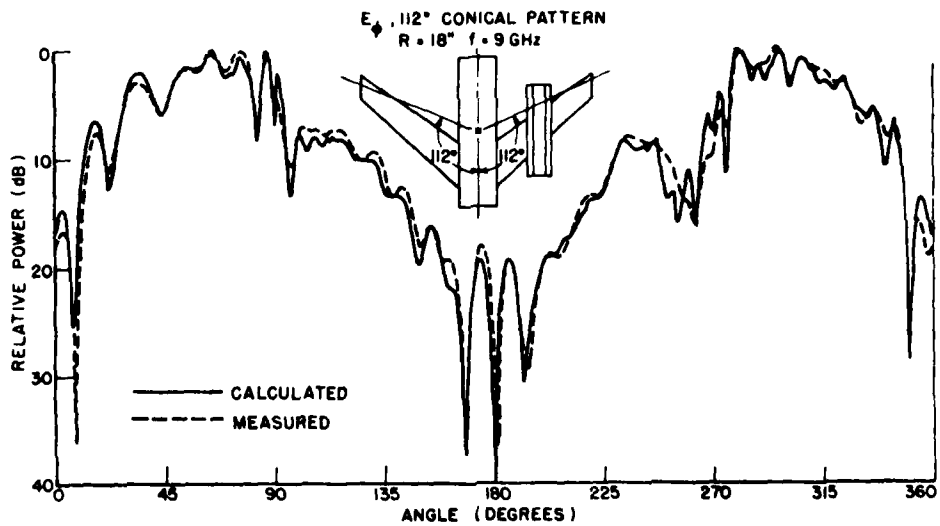


Figure 9. Comparison of measured and calculated near-field patterns for the test geometry. Note that the engine is simulated by flat plates.

Once the model is decided for the fuselage, the next step is to investigate the radiation from antennas on this doubly curved convex surface. This leads to the studies of radiation from sources on general perfectly conducting convex surfaces. This problem was treated previously for torsionless surface rays. Subsequently solutions were given for cylindrical and conical surfaces[3-5], where torsional surface rays exist. Under the present contract, the previous GTD solutions[3,4,5] were extended to obtain a uniform high-frequency solution for the radiation from apertures and monopoles which may excite torsional surface rays on a perfectly conducting, smooth, convex surface. The detailed analysis of this work was presented in the third quarterly report[6], only a brief summary is given here.

Consider a source located on a perfectly conducting convex surface at Q', as shown in Figure 10. The high-frequency solution described

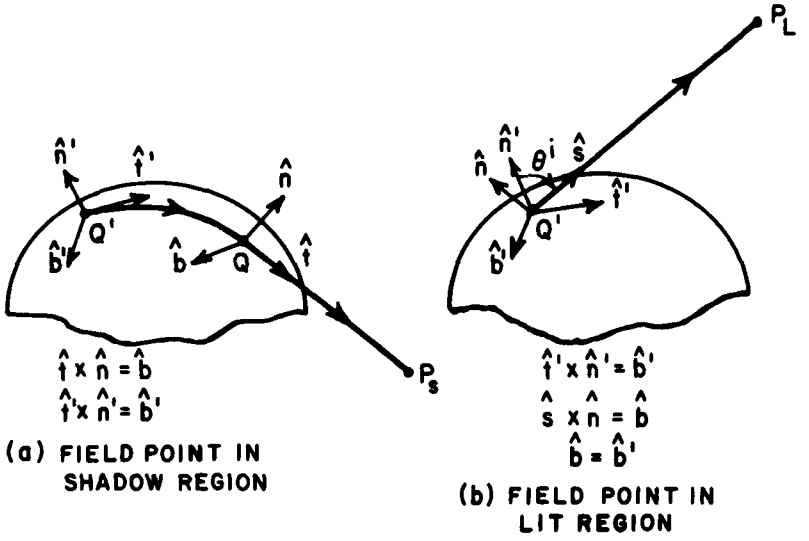


Figure 10. Rays emanating from a source on a convex surface.

here employes the ray coordinates of the GTD. Thus in the shadow region the radiation from Q' follows a surface ray to Q where it sheds tangentially from the surface to the field point $P_s$; whereas in the lit region, the radiation follows the incident ray of geometrical optics to $P_L$ in the direction of the unit vector $\hat{s}$. At Q the orthogonal unit vectors $\hat{t}$ and $\hat{n}$ (i.e., parallel to the ray and normal to the surface, respectively) are introduced along with the binormal unit vector ($\hat{b} = \hat{t} \times \hat{n}$). At Q' these same unit vectors are primed. In the lit region, $\hat{n} = \hat{b} \times \hat{s}$ where $\hat{b}' = \hat{b}$ is perpendicular to the plane of incidence.

The high-frequency electric field is given by $\bar{E} = \hat{n}E_n + \hat{b}E_b$ for points away from the convex surface in both the shadow and lit regions. Expressions for these field components have been deduced from a careful study of the cylinder and sphere conical problems in which higher order terms are retained in the asymptotic solutions; in addition, experimental results for sources on a spheroid were helpful in the generalization to the general convex surface.

Consider now a magnetic current moment $\bar{p}_m$ tangent to the surface at Q'. A complete description of this solution can be found in Reference 6, however, a simplified form is presented here.

In the lit region:

$$E_n \sim \frac{-jk}{4\pi}\left\{(\bar{p}_m.\hat{b}')(H^{\ell}+T_o^2 F\cos\theta^i)+(\bar{p}_m.\hat{t}')T_o\cos\theta^i F\right\}\frac{e^{-jks}}{s} + O(m_{\ell}^{-2}) \qquad (1)$$

$$E_b \sim \frac{-jk}{4\pi}\left\{(\bar{p}_m.\hat{b}')T_o F+(\bar{p}_m.\hat{t}')(H^{\ell}\cos\theta^i+F)\right\}\frac{e^{-jks}}{s} + O(m_{\ell}^{-2}, m_{\ell}^{-3}) \qquad (2)$$

In the shadow region:

$$E_n \sim \frac{-jk}{4\pi}(\bar{p}_m.\hat{b}')He^{-jkt}\left[\frac{\rho_g(Q')}{\rho_g(Q)}\right]^{1/6}\sqrt{\frac{d\psi_o}{d\psi}}\ \frac{e^{-jks}}{\sqrt{s(\rho_c+s)}} + O(m^{-2}) \qquad (3)$$

$$E_b \sim \frac{-jk}{4\pi}\left\{(\bar{p}_m.\hat{b}')T_oS+(\bar{p}_m.\hat{t}')S\right\}e^{-jkt}\left[\frac{\rho_g(Q')}{\rho_g(Q)}\right]^{1/6}\sqrt{\frac{d\psi_o}{d\psi}}\ \frac{e^{-jks}}{\sqrt{s(\rho_c+s)}} + O(m^{-2},m^{-3}) \qquad (4)$$

Note that $T_o = T\rho_g(Q')$;

$$m_\ell = \left[\frac{k\rho_g(Q')}{2(1+T_o^2\cos^2\theta^i)}\right]^{1/3}\ ; \quad m = \left[\frac{k\rho_g(q')}{2}\right]^{1/3}\ ; \quad F = \frac{S^\ell - H^\ell\cos\theta^i}{1+T_o^2\cos^2\theta^i}$$

in which T and $\rho_g(Q')$ are the surface ray torsion and radius of curvature at Q', respectively. In the lit region the various terms are found by projecting the incident ray onto the tangent surface at Q'. The quantities H, $H^\ell$, S and $S^\ell$ contain Fock type functions which depend upon the surface parameters at Q', and in the shadow region, upon the surface ray trajectory. The angles between adjacent surface rays at Q' and Q are $d\psi_o$ and $d\psi$, respectively and $\rho_c$ is the caustic distance at Q.[6]

In the monopole case, the expressions for the electric field in the lit region are given as

$$E_n \sim \frac{-jk}{4\pi}\sin\theta^i\left\{\frac{H^\ell+T_o^2\cos\theta^iS^\ell}{1+T_o^2\cos^2\theta^i}\right\}\frac{e^{-jks}}{s} + O(m_\ell^{-2}), \quad \text{and} \qquad (5)$$

$$E_b \sim \frac{-jk}{4\pi}\sin\theta^iT_oF\ \frac{e^{-jks}}{s} + O(m_\ell^{-2}); \qquad (6)$$

whereas, in the shadow region

$$E_n \sim \frac{-jk}{4\pi} He^{-jkt}\left[\frac{\rho_g(Q')}{\rho_g(Q)}\right]^{1/6} \sqrt{\frac{d\psi_o}{d\psi}}\ \frac{e^{-jks}}{\sqrt{s(\rho_c+s)}} + O(m^{-2}), \quad \text{and} \tag{7}$$

$$E_b \sim \frac{-jk}{4\pi} T_o Se^{-jkt}\left[\frac{\rho_g(Q')}{\rho_g(Q)}\right]^{1/6} \sqrt{\frac{d\psi_o}{d\psi}}\ \frac{e^{-jks}}{\sqrt{s(\rho_c+s)}} + O(m^{-2}) \ . \tag{8}$$

The previous expressions reduce to the geometrical optics field in the deep lit region and to the GTD creeping wave field in the deep shadow region. The expressions for the lit and shadow regions join smoothly at the shadow boundary. As expected, they reduce to the asymptotic solutions for the circular cylinder and sphere cases, but the higher order terms in "m" must be retained to pass smoothly to these two limiting cases. As the radii of curvature of the surface become infinite, $T_o = 0$ and Equations (1), (2), (5) and (6) simplify to the field of a current moment on a ground plane.

Now that the high frequency electric field is given in terms of the surface ray coordinate system (namely, a ray launches from the source Q' ) and traverses along the geodesic path to the shedding point Q , and then propagates along the tangent direction at Q toward the observation direction $\hat{r}(\theta_r,\phi_r)$; the major task remaining is to determine the unique geodesic path for a given radiation direction. This goal is accomplished and the detailed analysis is given in the second quarterly report[7], in which a numerically efficient and accurate scheme has been developed for determining the geodesic path in the case of an antenna radiating from a general convex surface of revolution. The surface of revolution is of interest in that it provides an analytical model for the aircraft fuselage structure. A computer program was also developed to solve the governing nonlinear equations using the secant (iteration) method. Some numerical results in terms of a family of geodesic curves are presented in Reference 7 for the case of sphere, prolate spheroid and cylinder.

Once the geodesic path is determined, one is ready to test the newly developed solutions (Equations 1-8) by applying it to calculate the radiation from slots and monopoles on perfectly conducting bodies. Some numerical results are obtained for the cases of an antenna radiating from circular and elliptic cylinders, cones and spheroids. In Reference 6, calculated results obtained by using the uniform GTD solutions are compared with the eigenfunction solution and/or experimental measurements and the agreement is excellent. Some examples are presented here. The patterns of a radial slot on a cone are shown in Figure 11 which

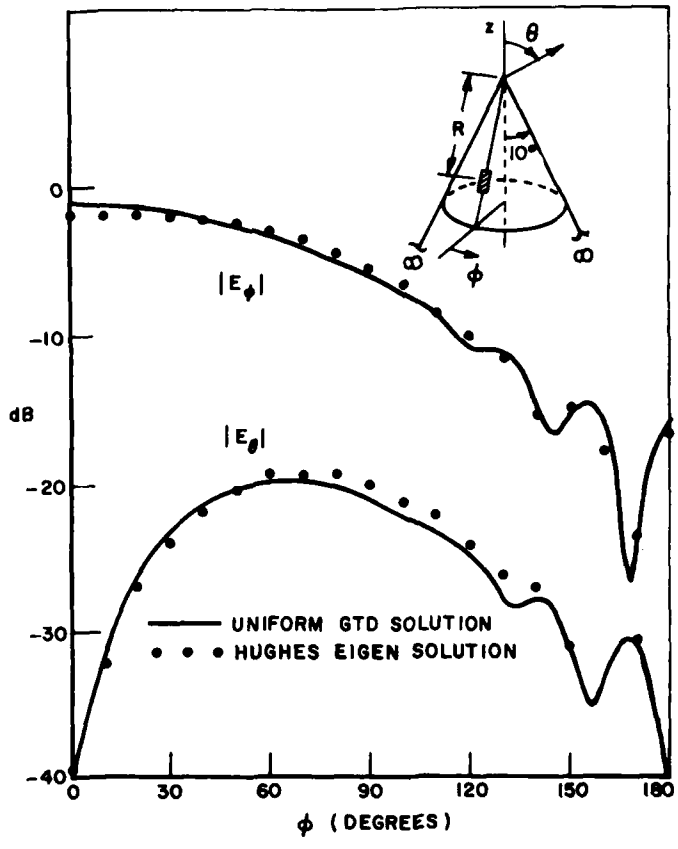


Figure 11. Radiation patterns of a radial slot in a cone.

compare very well with results obtained from an eigenfunction solution. In Figures 12 and 13, the patterns of a circumferential slot and monopole

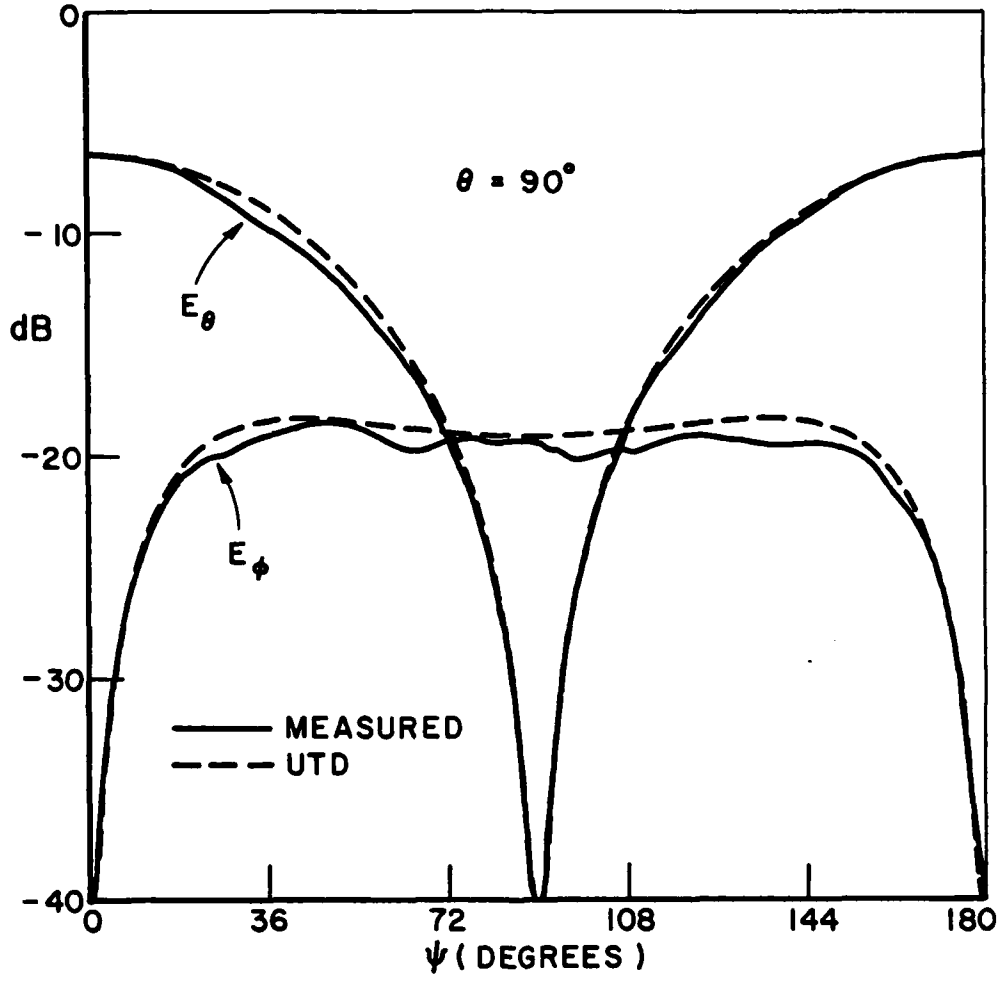


Figure 12. Radiation patterns of a circumferential slot in a conducting prolate spheroid.

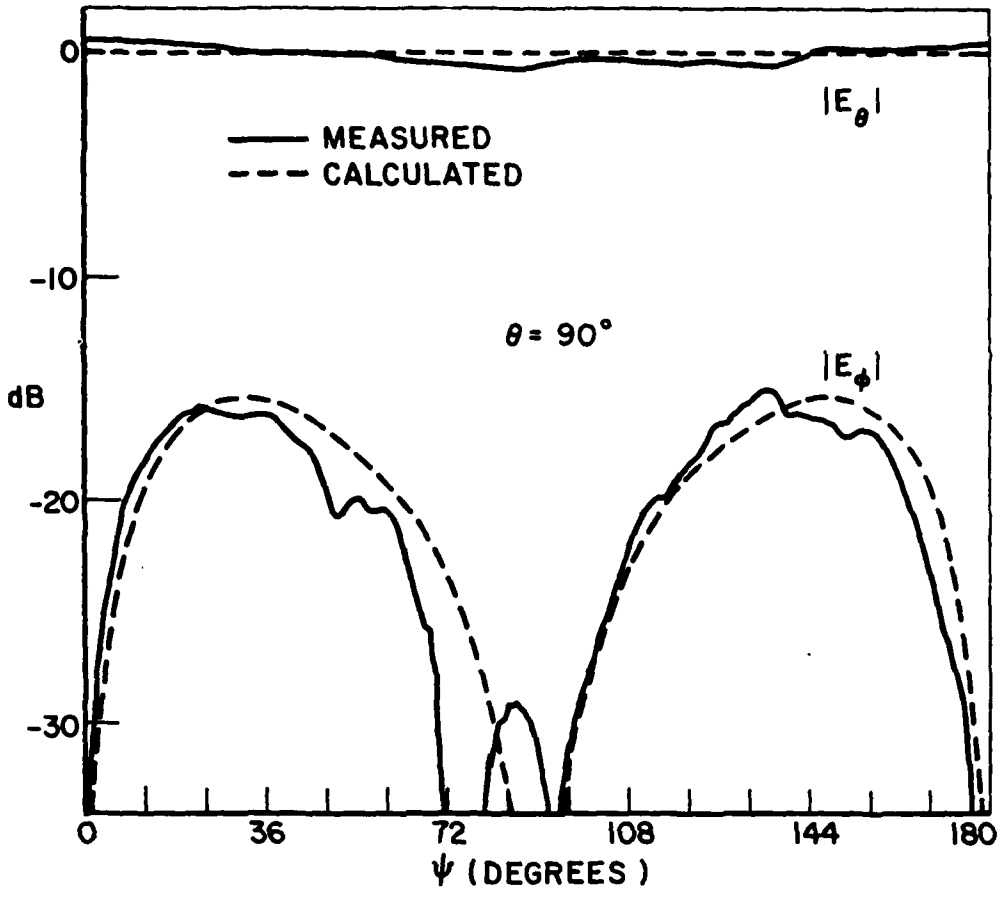


Figure 13. Radiation patterns of a monopole antenna on a conducting prolate spheroid.

are calculated and measured in the plane tangent to the spheroid at the source location. The prolate spheroid geometry is shown in Figure 14. Note that the $E_b$ component is due to the spheroid surface; it would vanish if the source were on a flat ground plane. Finally, a series of curves for the b-component of the electric field due to a circumferential slot on the spheroid are shown in Figure 15. Notice that the calculated and measured results are in very good agreement for the cases when the receiver is in the lit region ($\theta=74^0$), in the shadow boundary plane ($\theta=90^0$) and in the shadow region ($\theta=100^0$). This confirms the validity of the newly developed GTD solution for an antenna radiating from a conducting convex body.

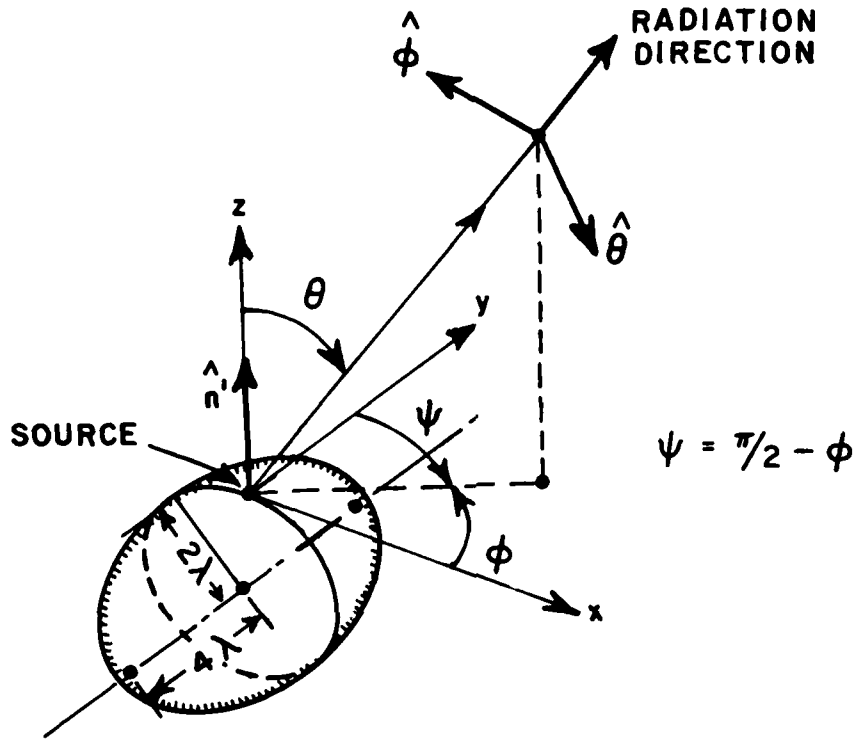


Figure 14. Prolate spheroid geometry.

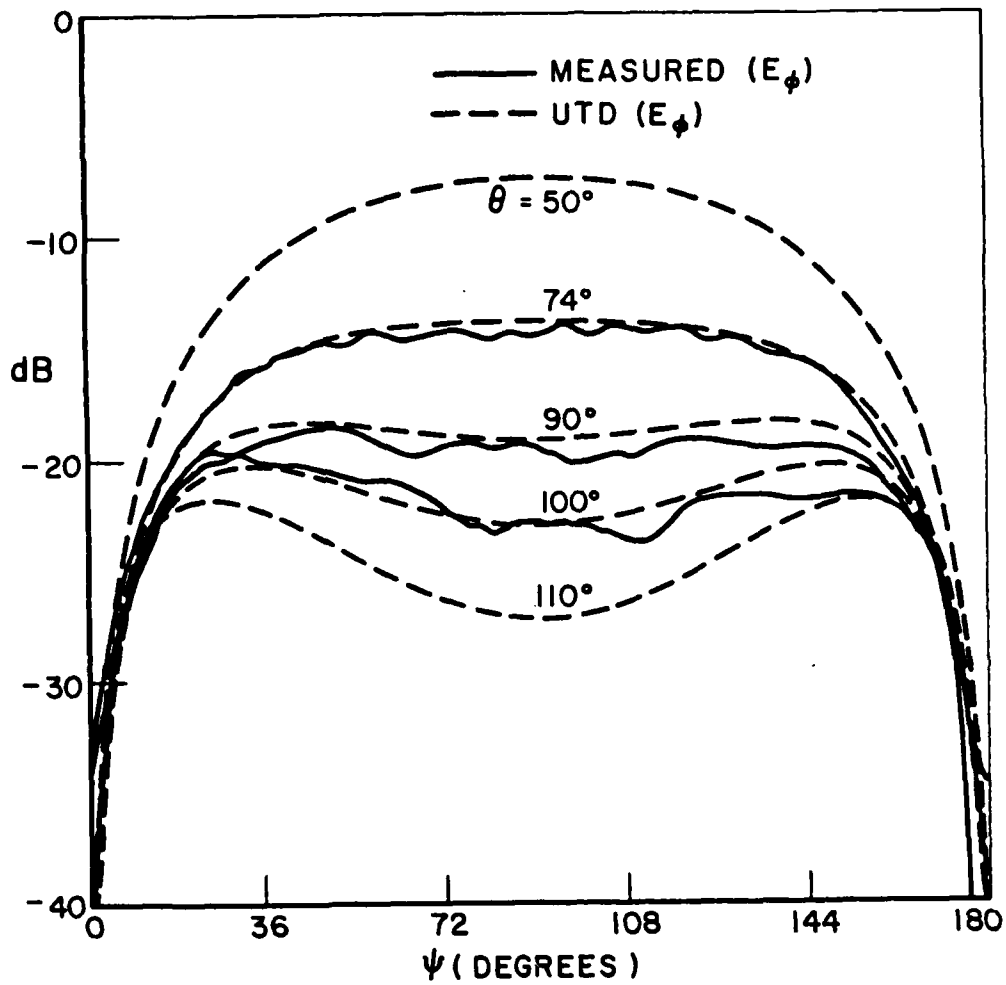


Figure 15. Radiation patterns of a circumferential slot in a conducting prolate spheroid.

## II. SIGNIFICANT ACCOMPLISHMENTS

A series of accomplishments have been made under the present contract. They are summarized below:

1. A paper entitled "Near Field Patterns Analysis for Airborne Antennas," has been accepted for publication by the IEEE *Transactions for Antennas and Propagation.*

2. An oral paper was presented at the 1978 International IEEE/AP-S Symposium at University of Washington; Seattle, Washington. The paper was presented in the session on high frequency diffraction and entitled "A Uniform GTD Solution for the Propagation from Sources on a Perfectly Conducting Convex Surface,"

3. A paper entitled "A *Uniform* GTD Solution for the Radiation From Sources on a Convex Surface" is under preparation and will be submitted for publication in the IEEE Transactions on Antennas and Propagation.

REFERENCES


1. W. D. Burnside, N. Wang and E. L. Pelton, "Near Field Pattern Computations for Airborne Antennas," Report 784685-4, June 1978, The Ohio State University ElectroScience Laboratory, Department of Electrical Engineering; prepared under Contract N00019-77-C-0299 for Department of the Navy, Naval Air Systems Command.

2. W. D. Burnside, N. Wang and E. L. Pelton, "Analysis of Aircraft Simulations Using Elliptic Cylinders and Multiple Plate," Report 711305-1, The Ohio State University ElectroScience Laboratory, Department of Electrical Engineering; in preparation under Contract N00019-78-C-0524 for Department of the Navy.

3. N. Wang, "Near Field Solutions for Antennas on Elliptic Cylinder," Report 784685-1, July 1977, The Ohio State University Electro-Science Laboratory, Department of Electrical Engineering; prepared under Contract N00019-77-C-0299 for Naval Air Systems Command.

4. A. Hessel, J. Shmoys and Z. W. Chang, "Surface Ray Analysis of Conformal Arrays," Final Report for Phase 2, POLY-EE/EP-75-149, Department of Electrical Engineering and Electrophysics, PINY, 1975.

5. S. Safavi-Naini and R. Mittra, "Source Radiation in the Presence of Smooth Convex Body," Electromagnetics Laboratory Technical Report No. 78-3, June 1978.

6. P. H. Pathak, N. Wang, W. D. Burnside and R. G. Kouyoumjian, "A Uniform GTD Solution for the Radiation from Sources on a Perfectly-Conducting Convex Surface," Report 711305-3, The Ohio State University ElectroScience Laboratory, Department of Electrical Engineering; being prepared under Contract N00019-78-C-0524 for Department of the Navy.

7. N. Wang and W. D. Burnside, "An Efficient Geodesic Path Solution for Prolate Spheroids," Report 711305-2, October 1979, The Ohio State University ElectroScience Laboratory, Department of Electrical Engineering; prepared under Contract N00019-78-C-0524 for Department of the Navy.